Improving Lattice QCD Calculation of the Collins-Soper Kernel

Artur Avkhadiev

in collaboration with
Phiala Shanahan, Michael Wagman, and Yong Zhao

INSTITUTE for NUCLEAR THEORY

Parton Distributions and Nucleon Structure

INT Workshop INT-22-83W

September 12–16, 2022

Fermilab

Argonne NATIONAL LABORATORY

TMD quantities probe non-perturbative physics

- Transverse motion of partons in hadrons gives rise to TMD functions in factorized cross-sections.
- **Together with evolution equations**, TMDs let us study hadronic structure and test SM physics.

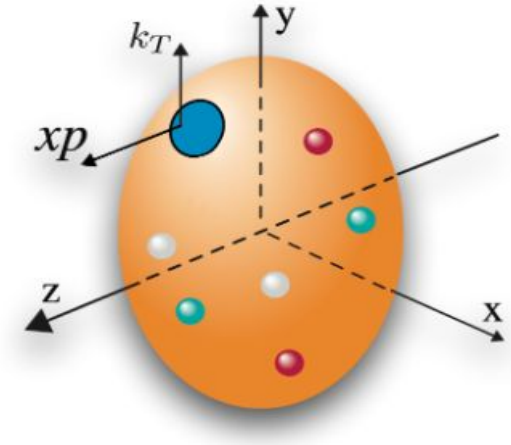

Fig. from TMD Handbook (modified).

Semi-Inclusive DIS

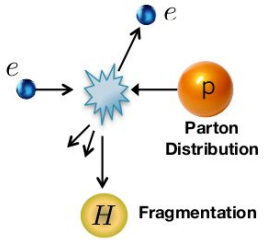

Drell-Yan

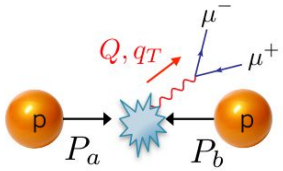

$q_T \ll Q$

Dihadron in e⁺e⁻

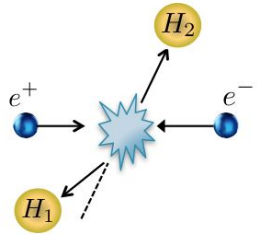

Fig. from TMD Handbook.

Collins-Soper (CS) kernel is important to the TMD program

- Renormalization of rapidity divergences in TMDs leads to the Collins-Soper scale ζ and the evolution equation

e.g. TMD PDFs in Drell-Yan:

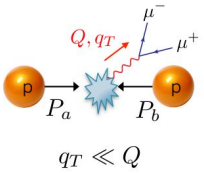

Fourier conjugate to parton's transverse momentum.

$$\zeta \frac{\mathrm{d}}{\mathrm{d}\zeta} \ln f_{i/h}(x, \mathbf{b}_\mathrm{T}; \mu, \zeta) = \frac{1}{2} \gamma^i_\zeta(\mu, b_\mathrm{T}).$$

Fourier-transformed TMD for parton *i* in hadron *h*.

Collins-Soper Kernel (independent of external state *h*).

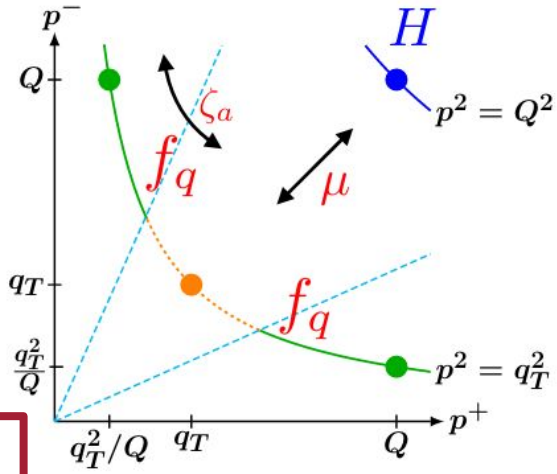

Fig. from Iain Stewart's talk at Lattice 2021.

- The CS kernel is thus required to
  - Sum large logarithms in ζ and
  - Relate TMDs at different Collins-Soper scales.

$$\zeta_a \zeta_b = Q^4$$

Artur Avkhadiev, MIT

The Collins-Soper (CS) kernel is non-perturbative

- Even if μ is perturbative, the CS kernel is non-perturbative at large b_{T}.
- The CS Kernel can be extracted from global fits to DY and SIDIS data, but non-perturbative modeling is significant for $b_{\mathrm{T}} \gtrsim 0.2\ \mathrm{fm}$.
- Non-perturbative CS kernel is a possible target for lattice QCD.

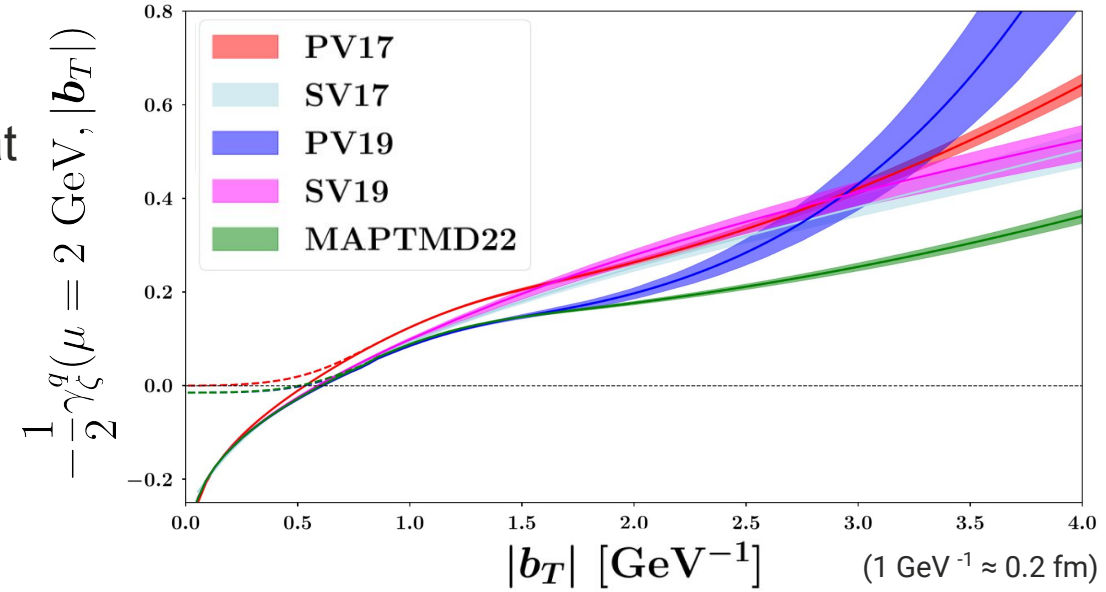

Fig. from Bacchetta et. al [MAP], 2206.07598 [style edited for clarity]

PV17 - Bacchetta et. al, JHEP 06, (2017), 1703.10157;
SV17 - Scimemi and Vladimirov, Eur. Phys. J. C78 (2018), 1706.01473;
PV19 - Bacchetta et. al, JHEP 07 (2020), 1912.07550;
SV19 - Scimemi and Vladimirov, JHEP 06 (2020), 1912.06532;
MAPTMD22 - Bacchetta et. al, 2206.07598.

LQCD can provide non-perturbative input for the CS kernel — but it has to be matched onto light-like correlations.

- Since $\zeta \sim Q^2 \propto \mathbf{P}^2$, γ_ζ may be defined through ratios of certain matrix elements with different external-state momenta P.
- These matrix elements are lightlike correlations of **staple-shaped operators** coming from factorization formulas — but in LQCD, only spacelike correlations of related operators can be computed. **Calculations must relate space-like and light-like correlations.**

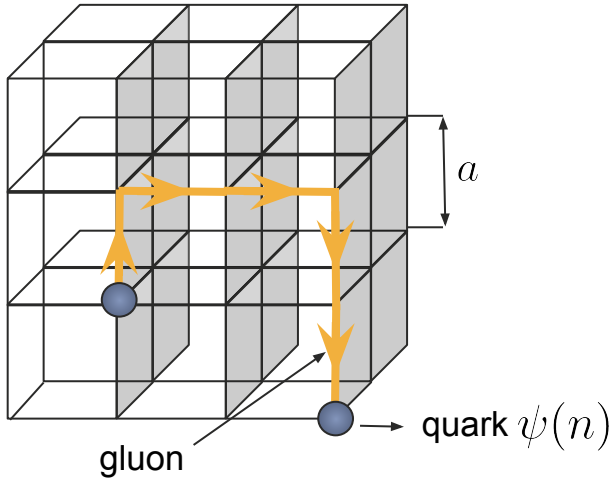

$$\langle \mathcal{O} \rangle = \frac{1}{Z} \int \mathcal{D}A \mathcal{D}\bar{\psi} \mathcal{D}\psi \exp(-S[A, \bar{\psi}, \psi]) \longrightarrow \langle \mathcal{O} \rangle \simeq \frac{1}{N_{\text{conf}}} \sum_k \mathcal{O}(U^{(k)}),$$

with field configurations $U^{(k)}$ distributed according to $\exp(-S[U])$.

Artur Avkhadiev, MIT

Extracting CS kernel from LQCD input at large momentum

Large Momentum Effective Theory (LaMET) provides a framework to match lightlike and boosted spacelike matrix elements, up to power corrections.

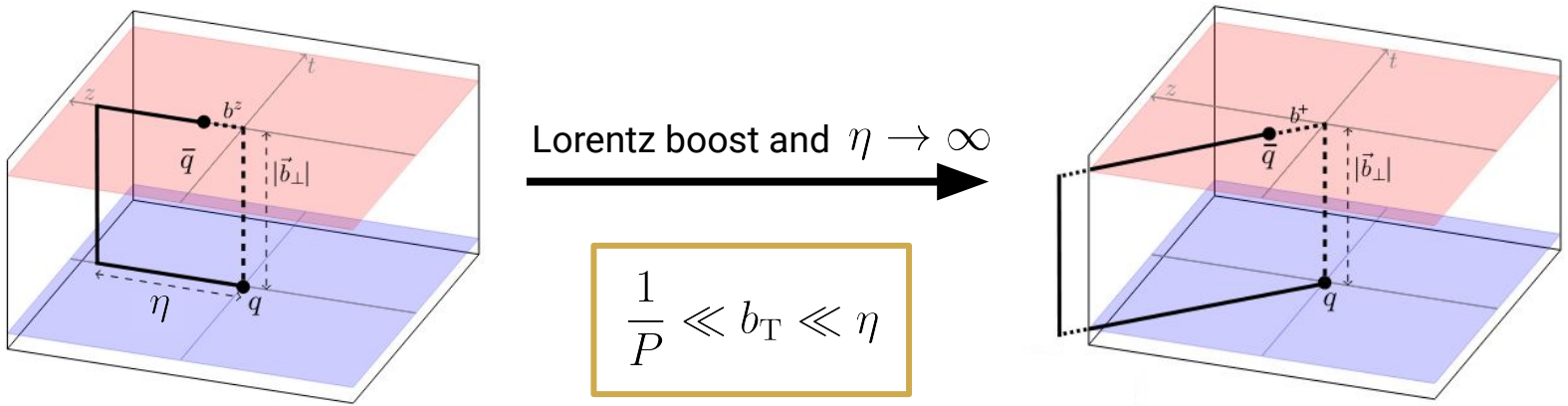

Fig. by Ebert, Stewart, Zhao, JHEP 1909 (2019)
(notation changed for consistency).

Ji, Sun, Xiong and Yuan, PRD91 (2015);
Ji, Jin, Yuan, Zhang and Zhao, PRD99 (2019);
Ebert, Stewart, Zhao, PRD99 (2019), JHEP09 (2019) 037;
Ji, Liu and Liu, NPB 955 (2020), PLB 811 (2020);
Vladimirov and Schäfer, PRD 101 (2020);
Ebert, Schindler, Stewart and Zhao, JHEP04 (2022) 178.

Two observables to compute the CS kernel with LQCD + LaMET

- Using **quasi-beam functions** from factorization formulas for cross-sections for processes such as Drell-Yan.
- The CS kernel is computed from ratios of beam functions.
- Beam functions are matched onto quasi-beam functions in LaMET.

$$\gamma_\zeta^q \propto \ln \frac{\tilde{B}(x, \mathbf{b}_\mathrm{T}, P_1)}{\tilde{B}(x, \mathbf{b}_\mathrm{T}, P_2)}$$

- Using **quasi-TMD wavefunctions** from the factorization formula for a form-factor of a large-momentum pseudoscalar meson.
- The CS kernel is computed from ratios of TMD wavefunctions (WFs).
- TMD WFs are matched onto quasi-TMD WFs in LaMET.

$$\gamma_\zeta^q \propto \ln \frac{\tilde{\psi}(x, \mathbf{b}_\mathrm{T}, P_1)}{\tilde{\psi}(x, \mathbf{b}_\mathrm{T}, P_2)}$$

space-like matrix elements computed in LQCD

Two observables to compute the CS Kernel with LQCD + LaMET

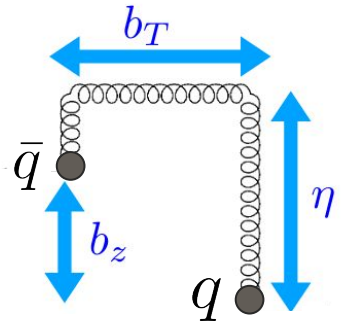

Fig. from Yong Zhao's Talk at CPHI-2022 (modified).

Both approaches involve staple-shaped operators,

$$\mathcal{O}_\Gamma(b^\mu, z^\mu, \eta) = \bar{q}(z^\mu + b^\mu)\frac{\Gamma}{2}\widetilde{W}(\eta; b^\mu; z^\mu)q(z^\mu)$$

in respective matrix elements computed in LQCD:

1. Quasi-beam functions with $\Gamma \in \{\gamma^z, \gamma^t\}$ from two- and three-point functions,

$$\tilde{B}_\Gamma(b^z, \mathbf{b}_\mathrm{T}, \eta, P^z) = \langle \pi(P^z)|\mathcal{O}_\Gamma(b^\mu, 0, \eta)|\pi(P^z)\rangle;$$

2. Unsubtracted quasi-TMD WFs with $\Gamma \in \{\gamma^z\gamma^5, \gamma^t\gamma^5\}$ from two-point functions:

$$\tilde{\psi}(b^z, \mathbf{b}_\mathrm{T}, \eta, P^z) \propto \langle 0|\mathcal{O}_\Gamma(b^\mu, -P^z, \eta)|\pi(P^z)\rangle.$$

Lower computational cost, especially at large momenta and physical masses.

Connecting bare spacelike matrix elements to the CS kernel

With bare matrix elements computed, their ratio yields the CS kernel after:

1. Renormalization;
2. $\eta \to \infty$ extrapolation;
3. Fourier Transform;
4. Perturbative Matching.

* Additional mixing may be induced by a renormalization scheme.
* Needs careful treatment of divergences.
* A major source of systematic uncertainty in the analysis.
* NLO effects are significant.

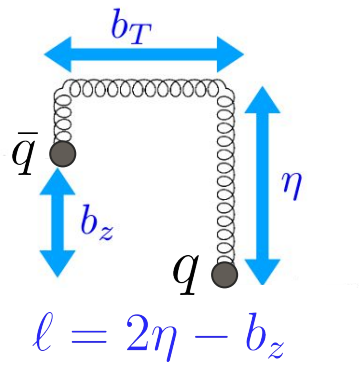

Fig. from Yong Zhao's Talk at CPHI-2022 (modified).

$$\gamma_\zeta^q(\mu, b_\mathrm{T}) = \frac{1}{\ln(P_1^z/P_2^z)} \ln\left[\frac{H(\mu, xP_2^z)}{H(\mu, xP_1^z)}\right.$$
$$\left. \times \frac{\int \mathrm{d}b^z e^{ib^z x P_1^z} P_1^z \lim_{\ell\to\infty} \tilde{\psi}_\pi^{\mathrm{ren.}}(\mu, b^z, \mathbf{b}_\mathrm{T}, \ell, P_1^z)}{\int \mathrm{d}b^z e^{ib^z x P_2^z} P_2^z \lim_{\ell\to\infty} \tilde{\psi}_\pi^{\mathrm{ren.}}(\mu, b^z, \mathbf{b}_\mathrm{T}, \ell, P_2^z)}\right]$$
$$+ \mathcal{O}\left(\frac{1}{(xP^z b_\mathrm{T})^2}, \frac{\Lambda_{\mathrm{QCD}}^2}{(xP^z)^2}\right)$$

Artur Avkhadiev, MIT

Systematic uncertainties in analyses are significant

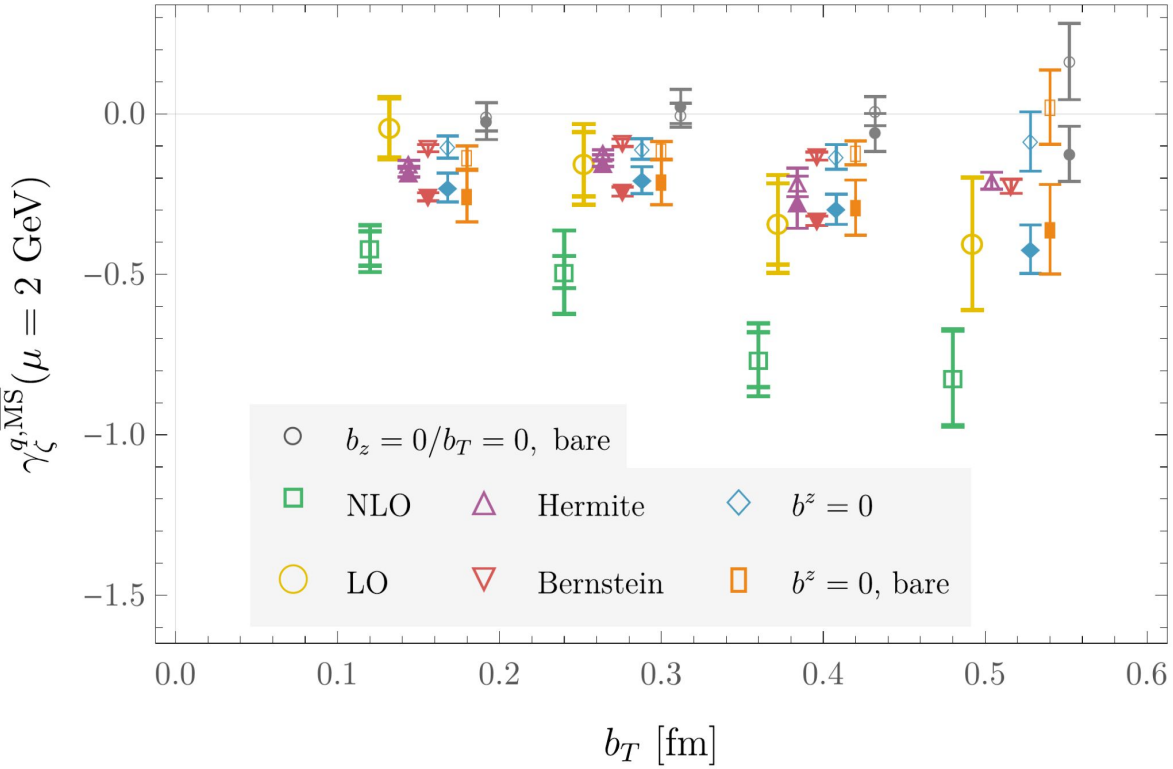

Fig. from Shanahan, Wagman, Zhao, Phys.Rev.D 104 (2021), 2107.11930

Same LQCD data with different treatments of matching, Fourier transform and renormalization leads to significant systematic effects and changes in uncertainty estimates.

$$\gamma_\zeta^q(\mu, b_{\rm T}) = \frac{1}{\ln(P_1^z/P_2^z)} \ln\left[\frac{H(\mu, xP_2^z)}{H(\mu, xP_1^z)} \times \frac{\int {\rm d}b^z e^{ib^z x P_1^z} P_1^z \lim_{\ell\to\infty} \tilde{\psi}_\pi^{\rm ren.}(\mu, b^z, \mathbf{b}_{\rm T}, \ell, P_1^z)}{\int {\rm d}b^z e^{ib^z x P_2^z} P_2^z \lim_{\ell\to\infty} \tilde{\psi}_\pi^{\rm ren.}(\mu, b^z, \mathbf{b}_{\rm T}, \ell, P_2^z)}\right] + \mathcal{O}\left(\frac{1}{(xP^z b_{\rm T})^2}, \frac{\Lambda_{\rm QCD}^2}{(xP^z)^2}\right)$$

LQCD calculations are broadly consistent. However:

Actions and systematics differ, and comparisons to phenomenology are preliminary. Further improvements are needed!

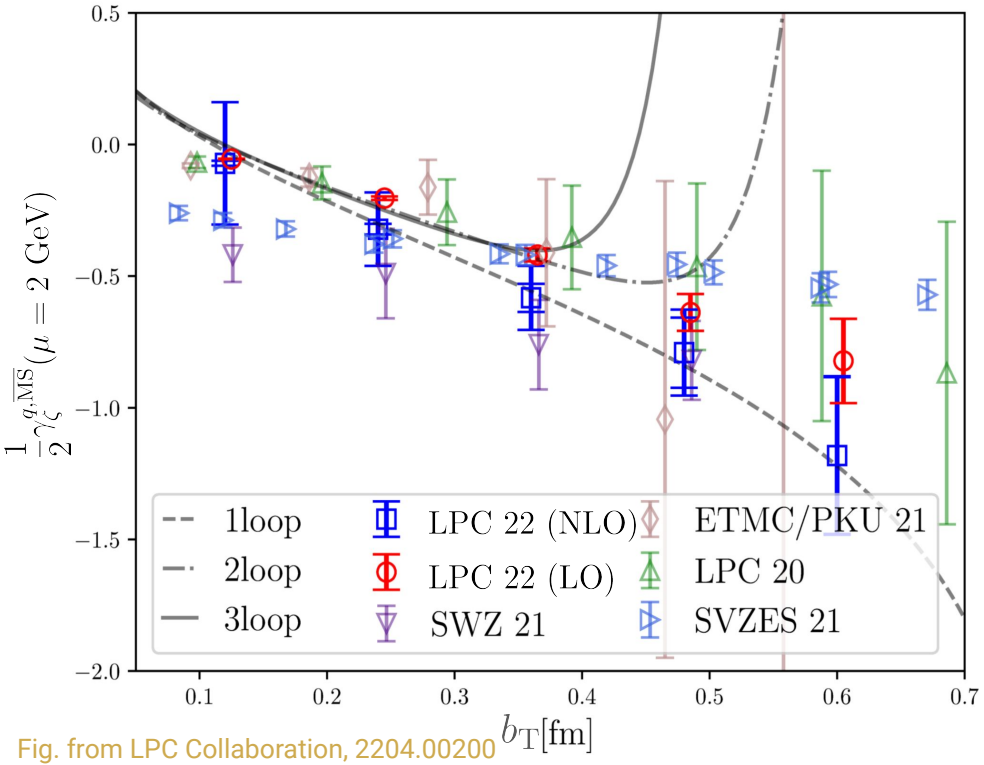

Fig. from LPC Collaboration, 2204.00200
[axes and legend labels modified]

Approach	Collaboration
Quasi-Beam Functions	**SWZ 21** PRD 104 (2021)
Quasi-TMD Wavefunctions	**LPC 20** PRL 125 (2020)
	ETMC/PKU 21 PRL 128 (2022)
	LPC 22 2204.00200
Mellin Moments of Quasi-TMDs	**SVZES 21** JHEP 08 (2021)

Observable	Collaboration	LQCD Setup	Matching	Fourier Transform	Operator Mixing
Quasi-Beam Functions	**SWZ 20** PRD 102 (2020)	$\frac{(m_\pi^{\text{val}})^2}{(P^z_{\max})^2} = 0.219$ *quenched*	LO	**Yes**	✔ (RI'-MOM)
	SWZ 21 PRD 104 (2021)	$\frac{(m_\pi^{\text{val}})^2}{(P^z_{\max})^2} = 0.129$	**NLO**	**Yes**	✔ (RI'-MOM)
Quasi-TMD Wavefunctions	**LPC 20** PRL 125 (2020)	$\frac{(m_\pi^{\text{val}})^2}{(P^z_{\max})^2} = 0.067$	LO	N/A	✔ (RI'-MOM)
	PKU/ETMC 21 PRL 128 (2022)	$\frac{(m_\pi^{\text{val}})^2}{(P^z_{\max})^2} = 0.063$	LO	N/A	✗
	LPC 22 2204.00200	$\frac{(m_\pi^{\text{val}})^2}{(P^z_{\max})^2} = 0.067$	**NLO**	**Yes**	✗
	This work (in progress)	$\frac{(m_\pi^{\text{val}})^2}{(P^z_{\max})^2} = 0.007$	**NLO**	**Yes**	✔ (RIx-MOM)
Mellin Moments of Quasi-TMDs	**SVZES 21** JHEP 08 (2021)	$\frac{(m_\pi^{\text{val}})^2}{(P^+_{\max})^2} = 0.035$	**NLO**	N/A	✗

Target improvements require increased computational efficiency

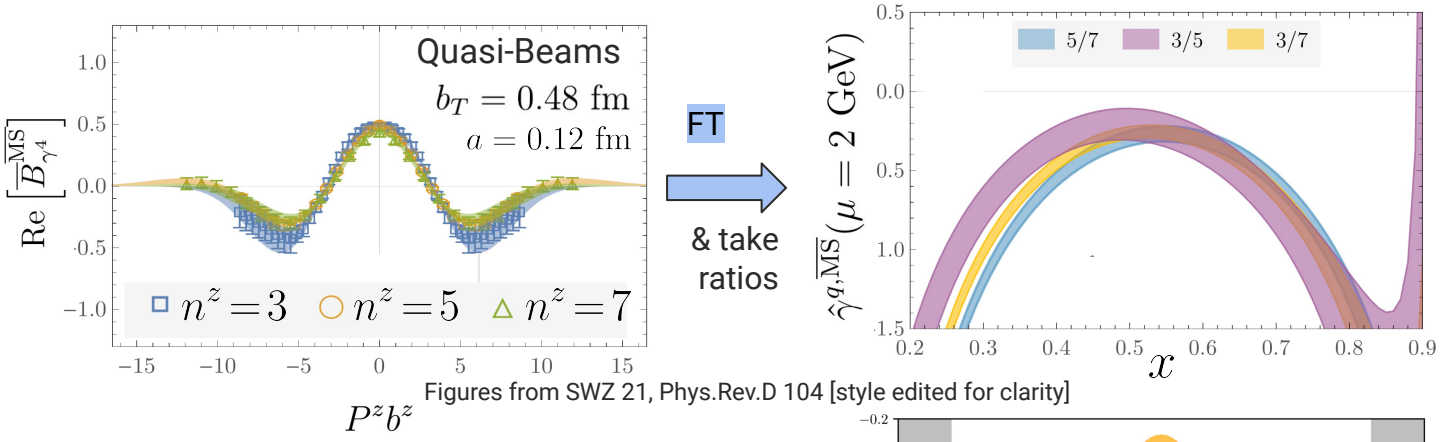

Figures from SWZ 21, Phys.Rev.D 104 [style edited for clarity]

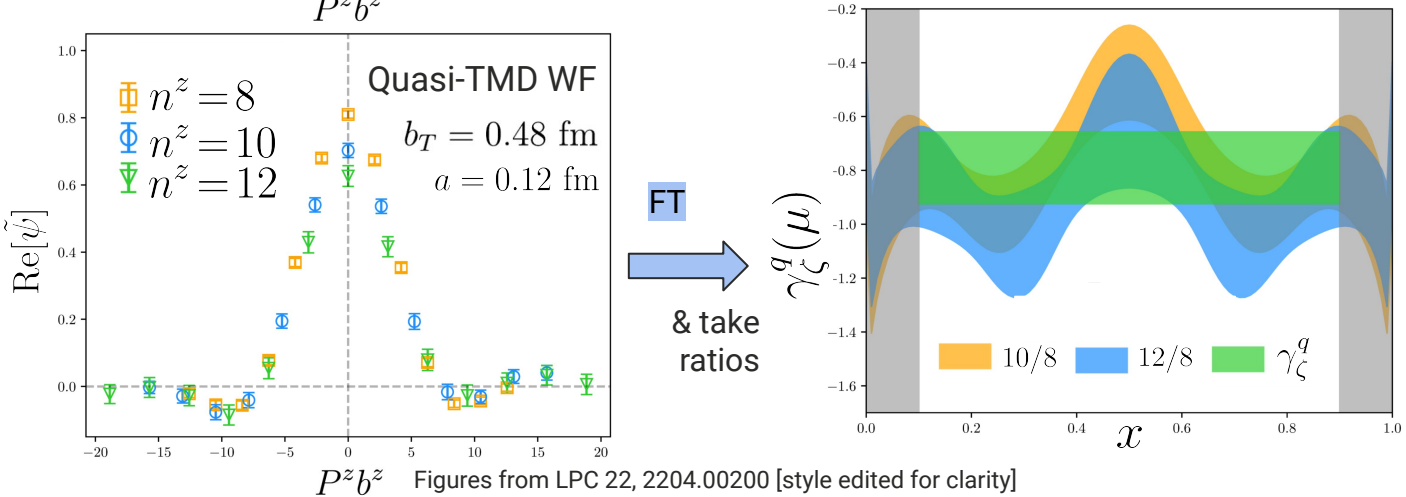

Figures from LPC 22, 2204.00200 [style edited for clarity]

- Reduce systematic uncertainties in the FT by increasing the range in $|P^z b^z|$.
- Use ~physical m_π^{val} to remove partial quenching and suppress power corrections.

These lead to greater computational costs.

Artur Avkhadiev, MIT

Recent developments increase computational efficiency

- Using TMD WFs instead of beam functions ⇨ only need two-point correlations.
- Staple configurations chosen for comparable truncation effects in the FT.
- New renormalization scheme reduces mixing *[see later slides]* ⇨ need to compute less gamma-matrix structures in bare matrix elements.
- Code optimization reduces computation wall time.

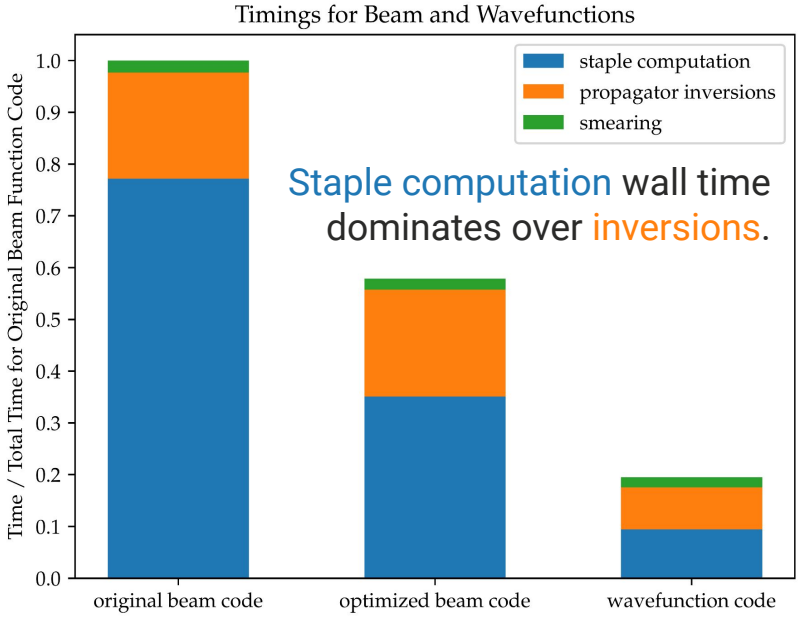

Estimate of fractional truncation effects based on SWZ 20

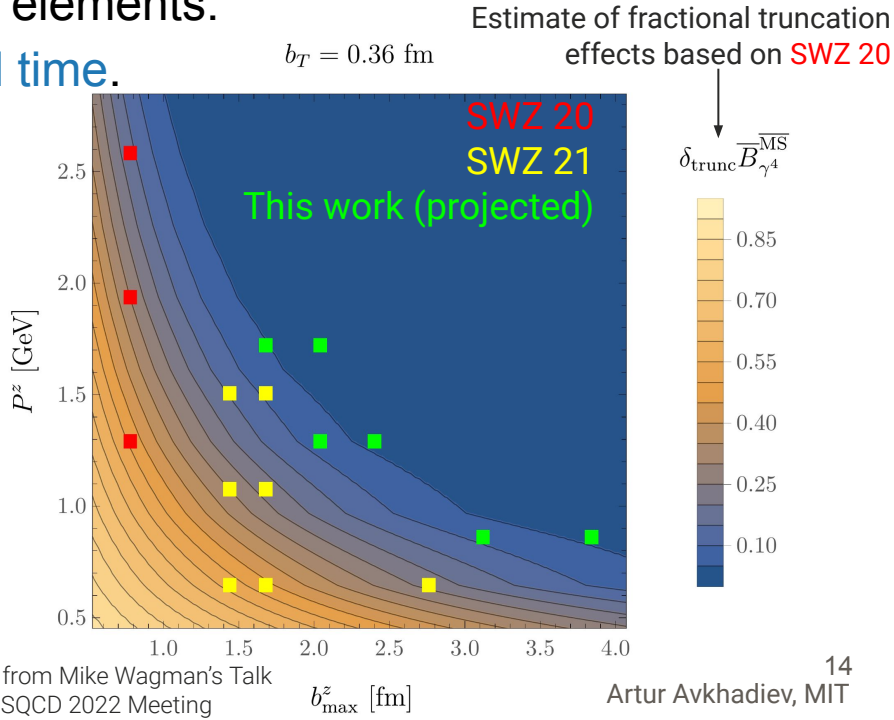

Fig. from Mike Wagman's Talk at USQCD 2022 Meeting

Aiming to improve systematics from the Fourier transform

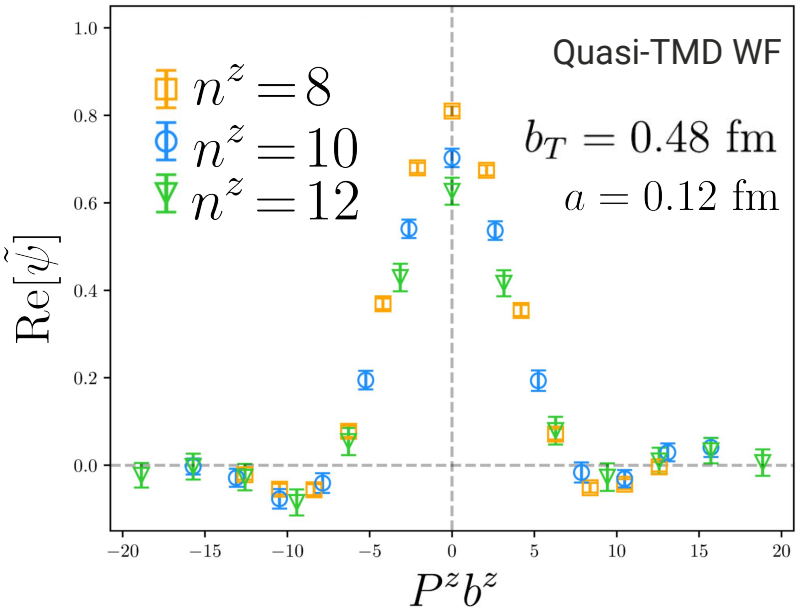

Figure from **LPC 22**, 2204.00200 [modified for clarity]

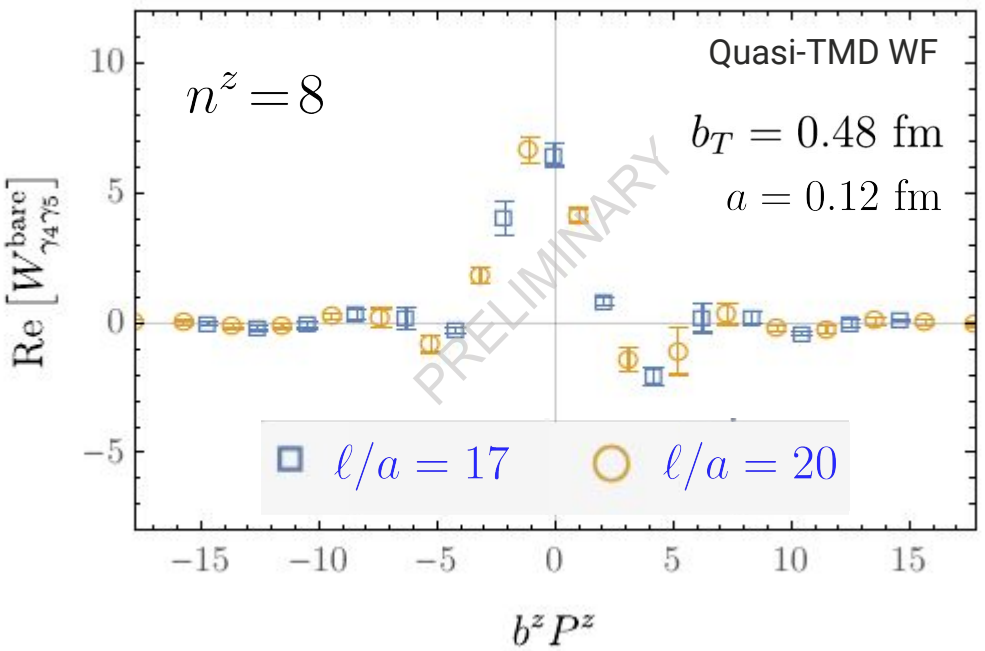

Preliminary figure from this work (different normalization)

The asymmetry in the bare wavefunction needs to be understood before taking the FT — mixing effects at play?

Using auxiliary fields for non-perturbative renormalization

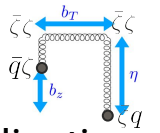

Get a renormalized **staple-shaped operator**

$$\mathcal{O}^{\text{ren.}}_{\ell,\Gamma} = Z^{\text{ren.}}_{\mathcal{O}_\ell\Gamma\Gamma'}\mathcal{O}^{\text{bare}}_{\ell,\Gamma}$$

By solving for Z_O in a renormalization scheme where it is given by matrix elements computed non-perturbatively, such as

$$\Lambda^{\text{bare}}_{\ell,\Gamma}(p,b) = \langle q(p)|\mathcal{O}^{\text{bare}}_{\ell,\Gamma}(b)|q(p)\rangle_{\text{gf,amp.}}$$

renormalized as

$$\Lambda^{\text{RI}'-\text{MOM}}_{\ell,\Gamma}(p,b) = [Z'_q(p)]^{-1} Z^{\text{RI}'-\text{MOM}}_{\mathcal{O}_\ell(b),\Gamma\Gamma'}(p)\Lambda^{\text{bare}}_{\ell,\Gamma}(p,b)$$

Set to its tree-level value at p = p_R, together with some renormalization condition for Z_q. This is **RI'-MOM**, *with a different Z_O for each staple configuration*.

[1]Green, Jansen, and Steffens, PRL 121 (2018) and PRD 101(2020).

With the auxiliary-field approach, renormalization of extended staples is simplified to that of point-like objects:

$$\begin{aligned}
&\bar{q}(b)\,\Gamma W_{-z}W_{\text{T}}W_{+z}\,q(0)\\
&\quad= \langle\bar{q}(b)\,\underbrace{\Gamma\zeta_{-z}(b)\bar{\zeta}_{-z}(\eta+b_{\text{T}})}_{W_{-z}}\underbrace{\zeta_{\text{T}}(\eta+b_{\text{T}})\bar{\zeta}_{\text{T}}(\eta)}_{W_{\text{T}}}\underbrace{\zeta_{+z}(\eta)\bar{\zeta}_{+z}(0)}_{W_{+z}}\,q(0)\rangle_\zeta\\
&\quad= \langle\underbrace{\bar{q}(b)\zeta_{-z}(b)}_{\phi_{-z}(b)}\,\Gamma\,\underbrace{\bar{\zeta}_{-z}(\eta+b_{\text{T}})\zeta_{\text{T}}(\eta+b_{\text{T}})}_{C_{-z,\text{T}}(\eta+b_{\text{T}})}\underbrace{\bar{\zeta}_{\text{T}}(\eta)\zeta_{+z}(\eta)}_{C_{\text{T},+z}(\eta)}\underbrace{\bar{\zeta}_{+z}(0)q(0)}_{\phi_{+z}(0)}\rangle_\zeta
\end{aligned}$$

where Wilson lines are given by zeta propagators in the extended theory, and Z_0 is broken down as

$$\begin{aligned}
\mathcal{O}^{\text{ren.}}_{\ell,\Gamma} &= e^{-\delta m(l+b_{\text{T}})}(Z^\dagger_{\phi_{-z}}\Gamma Z_{\phi_{+z}})\\
&\quad\times\langle\phi_{-z}(Z_{C_{-z,\text{T}}}C_{-z,\text{T}})(Z_{C_{\text{T},+z}}C_{\text{T},+z})\phi_{+z}\rangle_\zeta
\end{aligned}$$

with one renormalization condition for each Z, independent of staple configurations. This is **RI-xMOM**[1].

New renormalization scheme leads to reduced mixing effects

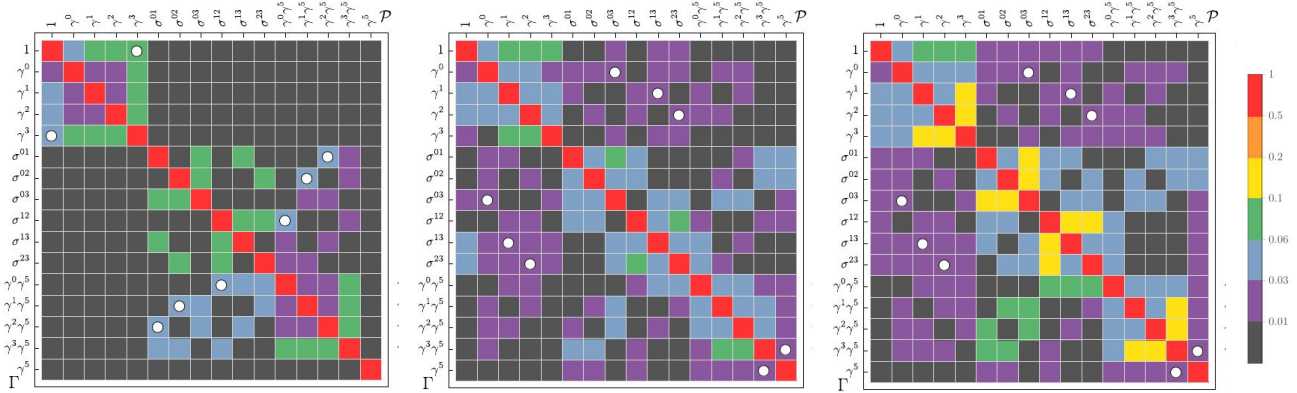

Figures from Shanahan, Wagman, and Zhao, PRD 101 (2020) *quenched*

Showing mixing patterns for **RI'-MOM** from left to right for: straight-line, symmetric, and asymmetric staples.

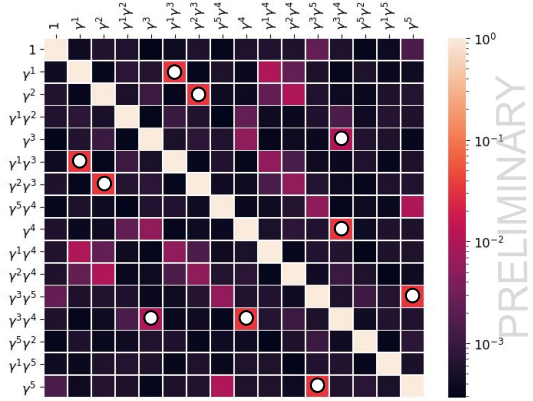

For short, straight-line configurations, mixing patterns in **RI'-MOM** agree with lattice perturbation theory at one-loop[1] (white circles), but deviations become large for staple-shaped Wilson lines; in comparison, mixing effects in **RI-xMOM** are well-controlled.

[1]Constantinou, Panagopoulos, and Spanoudes, PRD 99 (2019) and PRD 96 (2017).

Preliminary figure from this work (different ensemble and renormalization scale)

Summary and Outlook

- Determination of the Collins-Soper Kernel is critical to the TMD program.
- Non-Perturbative CS kernel can be determined with LQCD+LaMET.
- Further improvements are needed in LQCD calculations, which requires larger computational costs.
- Preliminary studies suggest quasi-TMD WFs will enable significantly more efficient CS kernel calculations.
- An improved quasi-TMD WF calculation is underway with NLO matching, robust non-local operator renormalization, and improved systematics in the Fourier transform at ~physical pion mass.

$$\gamma_\zeta^q(\mu, b_\mathrm{T}) = \frac{1}{\ln(P_1^z/P_2^z)} \ln\left[\frac{H(\mu, xP_2^z)}{H(\mu, xP_1^z)} \times \frac{\int \mathrm{d}b^z e^{ib^z x P_1^z} P_1^z \lim_{\ell\to\infty} \tilde{\psi}_\pi^{\mathrm{ren.}}(\mu, b^z, \mathbf{b}_\mathrm{T}, \ell, P_1^z)}{\int \mathrm{d}b^z e^{ib^z x P_2^z} P_2^z \lim_{\ell\to\infty} \tilde{\psi}_\pi^{\mathrm{ren.}}(\mu, b^z, \mathbf{b}_\mathrm{T}, \ell, P_2^z)}\right] + \mathcal{O}\left(\frac{1}{(xP^z b_\mathrm{T})^2}, \frac{\Lambda_\mathrm{QCD}^2}{(xP^z)^2}\right)$$

Backup

Figures from Shanahan, Wagman, Zhao, Phys.Rev.D 104 (2021), 2107.11930

Quasi-beam functions in RI'/MOM require asymmetry corrections

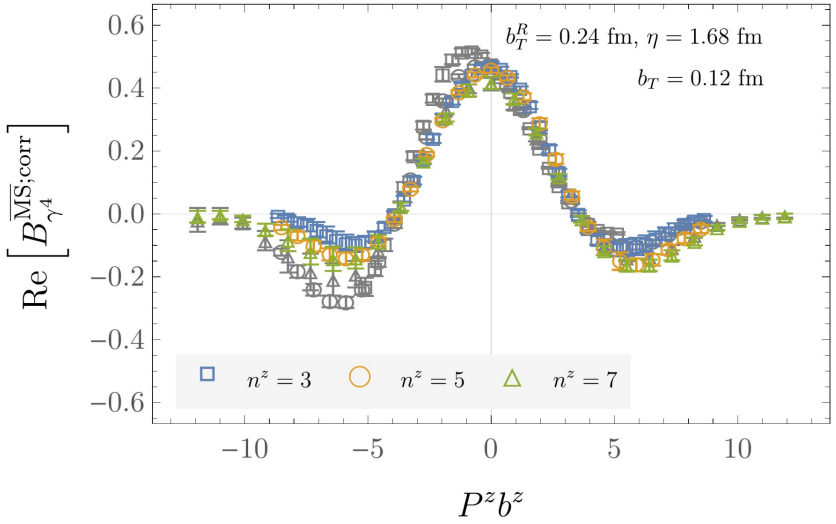

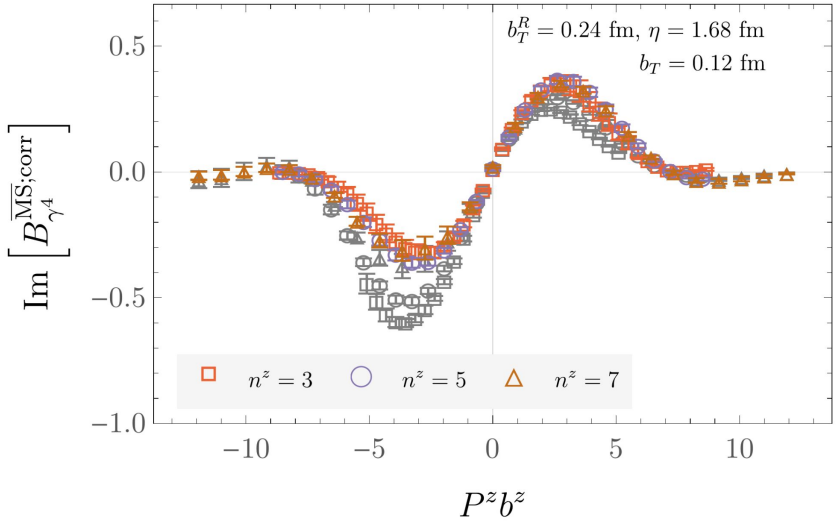

The observed asymmetries of beam functions in RI'/MOM could arise from an incomplete cancellation of linear divergence, show also in previous calculations:

Zhang et al [χQCD], PRD 104 (2021), 2012.05448
Huo et al [LPC], Nucl. Phys. B 969 (2021), 2103.02965

RI-xMOM seems to reduce the asymmetry in quasi-TMD wavefunctions.